

ORIENTATIONAL EFFECTS ON FATIGUE CRACK GROWTH RATES IN A FORGED DISC OF INCONEL 718 SUPERALLOY

S. Ponnelle^{1,*}, B. Brethes² and A. Pineau¹.

¹Centre des Matériaux P.M. Fourt, Ecole des Mines de Paris, UMR CNRS 7633
B.P. 87, 91003 Evry Cedex, France

²SNECMA - YKOM - Etablissement de Villaroche, 77550 Moissy Cramayel, France

*e-mail : sylvain.ponnelle@mat.ensmp.fr

ABSTRACT

Inconel 718 alloy is a material largely used for the fabrication of turbine discs working at elevated temperature (up to 600°C). The fabrication route used involves several thermomechanical operations of forging and circular rolling, which result in a strong microstructural orientation of the material and especially of the distribution of δ phase and carbide particles (here called Forming Induced Arrangement). Fatigue Crack Growth Rates (FCGR) were measured on specimens cut from an industrial disc along various crack orientations. Two types of specimens were used, conventional CT specimens ($W=40\text{mm}$) and smaller KB specimens containing a small 3D semi-elliptical EDM notch (0.3mm). These specimens were tested at 650°C under creep fatigue conditions.

Large differences were observed between the various orientations of crack front according to FIA.

It is shown that the FCGR are the higher when the crack front is parallel to the microstructural layers whereas slower rates are measured when the crack front is perpendicular to them. Moreover, no significant hold time effects were observed along this latter direction. S.E.M. fractographic observations showed that the fracture mode is predominantly intergranular when FCGR are the higher and essentially transgranular when the crack propagates along the other direction (where no hold time effect is noticed). 3D effects observed on small KB specimens are discussed according to arrangement of the aspect ratio of the semi-elliptical cracks. Final conclusions about suitable arrangement of δ phase in components are drawn.

1 INTRODUCTION

Some of the most critical components in aeronautical engine are turbine discs which can be exposed to high stresses (up to 1000 MPa) and to temperature close to 650°C. Thereby, nickel based superalloys are usually used for the fabrication of these discs because of their good mechanical properties at elevated temperature. Among them, Inconel 718 is a largely used alloy because of its good formability and weldability properties. One of the main specifications needed for this alloy for this application is a good resistance to fatigue crack growth (FCG). Many studies have focused on this point and major influencing parameters on fatigue crack growth rates (FCGR) can be listed as following [1,2,3] :

- *Material variables*: i) chemical composition, ii) grain morphology and grain size, iii) morphology and size of γ' and γ'' strengthening precipitates, and iv) capacity of stress relaxation and, more generally, material mechanical behaviour.

- *Environmental and mechanical variables:* i) temperature, ii) frequency and waveform of fatigue cycle, iii) creep-fatigue interaction, and iv) environmental effects and particularly oxidation effects.

Emphasis should be laid on fracture modes depending upon temperature and cycle frequency [4]. Three fracture modes can be observed on 718 alloy. At low temperature and high frequency, fracture is fully transgranular and FCGR is relatively low, depending only on the cycle amplitude ("cycle dependent" mode). On the opposite, at high temperature and low frequency, fracture mode is fully intergranular and FCGR is particularly high, depending on the time exposed at high load. This fracture mode is called "time dependent". Differences in FCGR of up to two orders of magnitude can be measured between the two modes. Finally, stands the mixed mode regime between these two extreme conditions, corresponding to intermediate FCGR. As a rule, creep-oxidation-fatigue interactions at elevated temperatures (~650°C) lead to FCGR behaviour which is time dependent.

Most of these previous studies used laboratory materials such as bars or plates, with various heat treatments. The fabrication route used for discs involves several thermomechanical operations of forging and circular rolling which result in a strong orientation of the microstructural details (see material section). Very few results based on industrial components and considering anisotropy of FCGR due to microstructural effects have been reported. However, Pédrón and Pineau [5] showed the influence of a number of microstructural effects using specimens cut from a rolled ring of alloy 718. The authors have concentrated on the effect of grain size. At 650°C, for creep fatigue conditions (5 min hold-time at maximum load), FCGR was shown to be higher for small grains than for coarse ones, best results being obtained on a duplex microstructure. The other conclusion is that FCGR is significantly reduced when the crack front is oriented perpendicularly to the rolling direction compared to a crack orientated along this direction.

This paper presents some results of an on going study of FCGR at 650°C in an industrial forged disc of Inconel 718 alloy, as regards crack front position related to microstructural orientations, pointing out strong anisotropy effects.

2 MATERIAL

2.1 General characteristics

All the specimens of this study were cut from a forged turbine disc produced by SNECMA. The fabrication route starts from a triple melted billet (VIM - VAR - ESR). The chemical composition is given in TABLE 1. The forming of the disc consists of a sequence of forging and circular rolling and final die stamping at different temperatures. Conventional heat treatment is then applied consisting in a first treatment at 955°C for 1 h followed by air cooling, then in an ageing treatment at 720°C for 8 h, followed by furnace cooling down to 620°C, and final ageing at 620°C for 8 h before air cooling. These treatments lead to a fine grained austenitic γ matrix (ASTM 9-10), strengthened by the precipitation of γ' ($\text{Ni}_3(\text{Ti-Al})$, FCC, 20 nm spheres) and γ'' ($\text{Ni}_3(\text{Nb-Ti})$, BCT, 20 nm discs). Volume fraction of γ'' precipitate is about 15%.

| Ni | C | Cr | Fe | Mo | Nb | Ta | Ti | Al |
|---------|------|-------|-------|------|------|------|------|------|
| balance | 0.03 | 17.94 | 18.00 | 2.97 | 5.27 | 0.01 | 1.01 | 0.46 |

TABLE 1 : CHEMICAL COMPOSITION OF INCONEL 718 DISC STUDIED (WT %)

A third type of precipitate is also present in the alloy, the orthorhombic Ni_3Nb δ phase, figure 1. Two populations of δ phase can be observed. Particles with very fine platelet morphology (thickness < 0.1 μm) are found along grain boundaries or arresting annealing twins inside grains. Bigger cellular δ particles are found both at grain boundaries and inside the grains. These precipitates look like ellipsoid discs, 1 to 5 μm long and around 0.5 μm thick. δ phase is measured to occupy about 4 % of the surface.

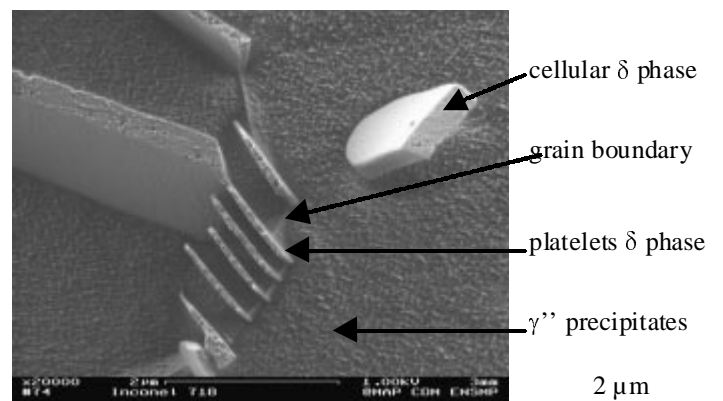


FIG. 1 : THE TWO SPECIES OF δ PHASE

The last species of particles present in the alloy are carbides and nitride-carbides with a size from 1 to 10 μm , precipitating essentially at grain boundaries. The percentage of these carbides on surface observation is about 0.3%.

2.2 Forming Induced Arrangement (FIA)

The main difference between a simple forged bar and an industrial component such as a turbine disc lies in the flow pattern of the material. Carbides and δ particles are present in the material before or during forming operations, depending on involved temperatures. Hence their arrangement into the industrial part will follow

the mechanical deformations undergone by the material. This is what we call the Forming Induced Arrangement (FIA). Figure 2 reproduces the schematic flow pattern (or FIA) of the disc. Two scales of microstructural arrangement give the observation of flow pattern. The first scale is related to carbide alignment, which can be seen at low magnification after mechanical polishing, before etching. The second scale is related to the cellular δ phase arrangement. Fig. 2c reproduces disposition of δ discs according to the three directions of the component in the marked extracted volume (Fig 2a). Image analysis of face r - z of the cube reveals principal orientation of a majority of ellipsoid discs according to macroscopic FIA. Observations on face θ - z indicate the same trend whereas no particular orientation is found for r - θ face. Hence, the disposition of cellular δ phase can be compared to sheets of discs reflecting the history of component deformation during forming. Next sections show the influence of the position of the crack front according to the sheets of δ on the FCGR.

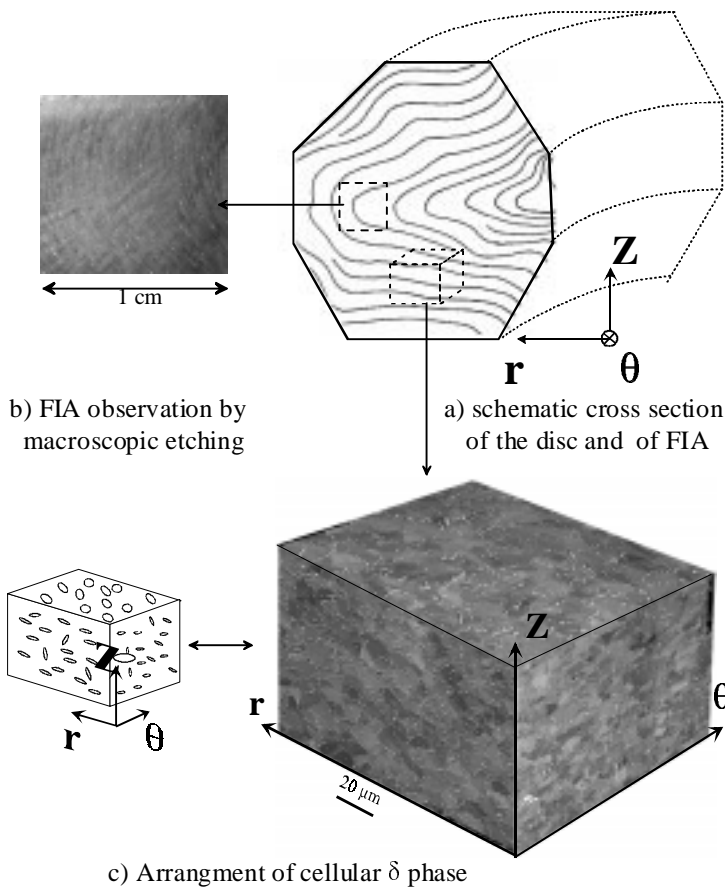


FIG. 2 : CHARACTERISTICS OF FORMING INDUCED ARRANGEMENT

3 FCGR IN INCONEL 718 DISC

3.1 Experimental procedure of FCGR measurements

3.1.1 Specimens

Two types of specimens were used for this study.

A first series of data was obtained from conventional CT specimens, 10 mm thick and 40 mm wide ($B=10\text{mm}$, $W=40\text{mm}$). For this kind of specimen, the crack front can be considered as a 2 dimensional (2D) feature.

Other series of data were collected from KB 2.5 specimens (fig. 3). These specimens can be described as plates of section $t \times 2w$ (2.5×8.3 mm) containing a halfpenny shape initial defect of 0.3 mm radius, performed by electro-discharge machining. Hence, the crack can be considered as a 3 dimensional (3D) problem. For this geometry, SIF is calculated from Newman and Raju equations [6], modified for crack aspect ratio > 1 .

3.1.2 Test procedures

During the test, crack growth is measured by DC Potential Drop technique (DCPD) for both types of specimens. Each specimen is fatigue pre-cracked at room temperature at high frequency (20 to 40Hz) under

sinusoidal wave cycles with a positive load ratio of $R=0.1$. As the crack is initiated and propagates, the applied load is progressively reduced to reach the following prescribed conditions. For CT specimens, pre-cracking ends with a crack of an average length of 13 mm and $\Delta K \sim 15 \text{ MPa}\sqrt{\text{m}}$. For KB 2.5 specimens, pre-cracking ends with a measured edge crack of $2c = 1 \text{ mm}$, and ΔK around $13 \text{ MPa}\sqrt{\text{m}}$. Pre-cracking is then finished at high temperature (650°C) by initiating crack growth under triangular cycles of 20s until 0.1 mm of propagation for KB specimen and 1mm for CT specimen is reached.

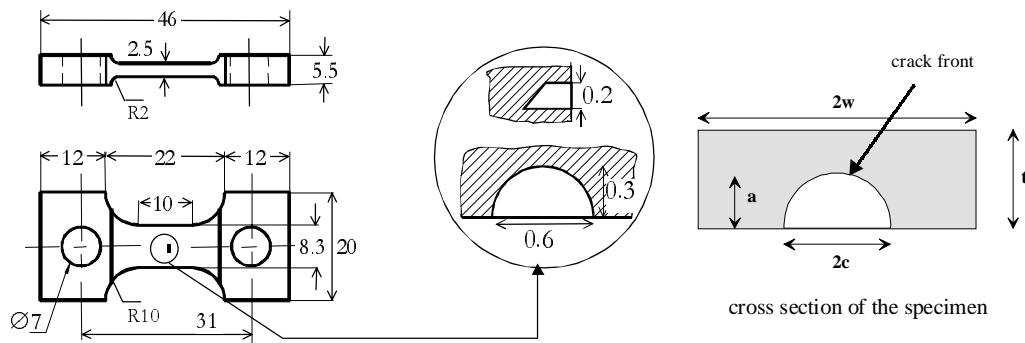


FIG. 3 : KB 2.5 SPECIMEN GEOMETRY WITH ITS INITIAL SEMI-CIRCULAR DEFECT.

The FCGR tests are then conducted at 650°C with a stress ratio of $R=0.1$, maximum load being constant at each cycle. Two types of cycles are applied : fatigue triangular cycles of 20s (called 10-10 cycles) and creep fatigue trapezoidal cycles with the same rate of loading and unloading than the previous ones and a 300s hold time at maximum load referred to as 10-300-10 cycles. During the test, beach marking was made by switching from one type of cycling to another or by a short crack growth at room temperature. After the test, each specimen is fully opened and beach marks are used to correct possible unmatched on DCPD crack length evaluation and aspect ratio α .

3.1.3 Specimen extraction

Figure 4 reproduces positions of specimen extraction from the component and the position of the crack front regarding FIA. CT specimens were used to study 2D radial cracks while KB 2.5 specimens were used to measure FCGR in other directions.

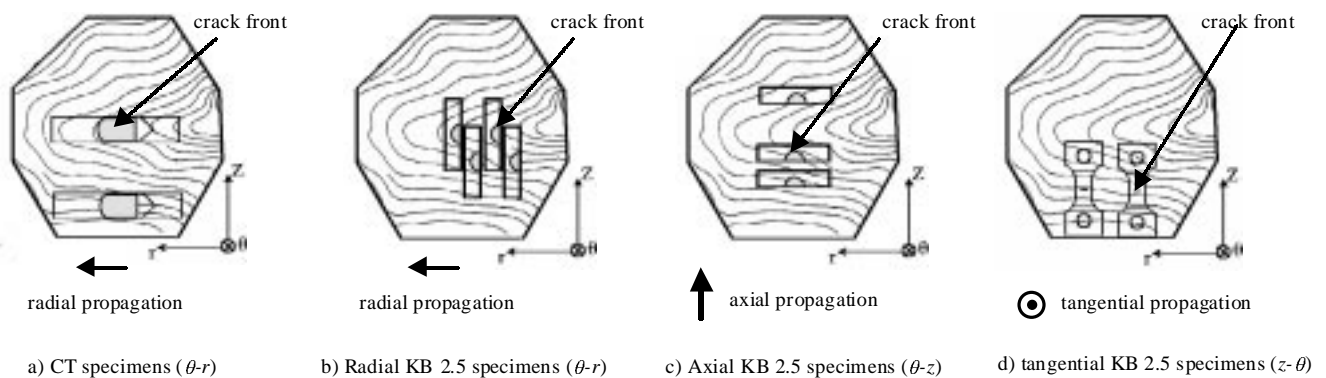


FIG. 4 : EXTRACTION POSITION OF SPECIMENS AND POSITION OF THE CRACK FRONT COMPARED TO FLOW PATTERN.

3.2 Radial FCGR on CT specimens

Results on CT specimens are plotted in Fig 5a for fatigue conditions (10-10) and creep-fatigue conditions (10-300-10). Specimens extracted on position A exhibit a large hold time effect. FCGR is about 80 times larger compared to 10-10 fatigue conditions, which is in good agreement with what is usually observed on this material [1-5]. On the other hand, B type specimens produce very low FCGR for 10-300-10 cycles. It is worth noting that, for this extraction localisation, FCGR is the same with or without applying a 5-min hold time at maximum load. Figure 5b reproduces the cross section along the crack path of two typical specimens. As expected, the specimens which produce high sensitivity to hold time present fully intergranular fracture. Conversely, when no hold time effect is measured, fracture mode is mixed, locally intergranular with large proportion of transgranular fracture. The same fracture mode is observed with 10s-10s triangular pure fatigue cycles. Hence, FCGR behaviour is directly linked to fracture modes.

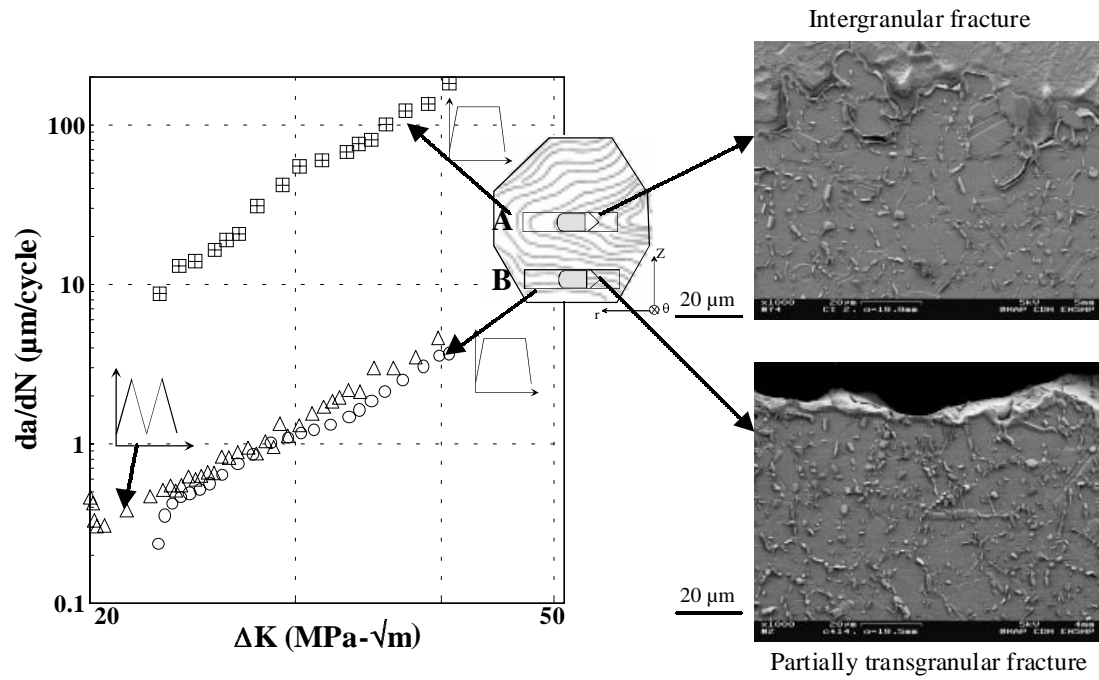


FIG. 5 : (A) FCGR AT 650°C MEASURED ON CT SPECIMEN AND (B), FRACTURE MODES

3.3 FCGR on KB 2.5 specimens

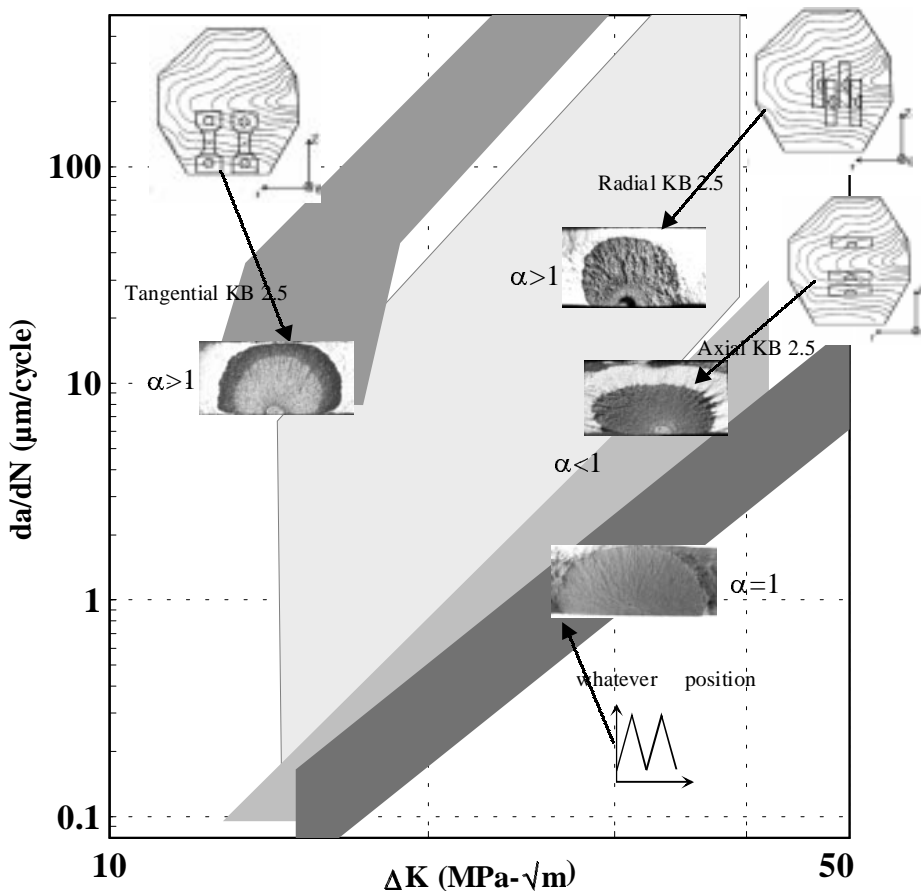


FIG. 6 : FCGR AND CRACK FRONT SHAPE FOR KB 2.5 SPECIMEN DEPENDING UPON EXTRACTION POSITION. CREEP - FATIGUE À 650°C.

Figure 6 summarises the results obtained on KB 2.5 specimens, depending upon specimen extraction and crack front aspect ratio α . The extraction position of specimens seems to play a major role on the observed scatter.

Tangential direction KB 2.5 specimens seem to produce the higher rates of crack propagation with a large hold time effect. On the other hand, for the same macroscopic loading and stress ratio, axial KB specimens lead to very low growth rates. For this orientation, very slight differences in FCGR are measured between pure fatigue and creep fatigue cycles. Concerning radial direction KB specimens, the scatter band is larger. Some specimens exhibit high hold time effect while others very slight effect. Finally, for pure fatigue conditions, all the data can be plotted within a factor 3 scatter band, whatever the direction of propagation. Simply note that

tangential orientated cracks produce the higher rates in this scatter band.

Concerning fracture modes, the same comments as those on CT specimens can be made. Fracture is fully intergranular when the higher rates are produced, proportion of transgranular cracking being more and more

important with the decrease of FCGR until reaching the same aspect of pure fatigue conditions (10s-10s cycles). Next section will show more details on fracture modes for the high rates of crack propagation. Another comment should be made about the crack aspect ratio. For pure fatigue conditions (10s-10s cycles), the crack front is very close to a semi-circular shape, $\alpha=a/c\sim 1$. For creep fatigue conditions, specimens that produce low FCGR exhibit semi-elliptical shape with $\alpha<1$, close to 0.8. On the contrary, a tunnelling effect leading to $\alpha>1$, up to 1.3 for some cases is observed at high crack growth rates.

4 DISCUSSION

4.1 2D CT specimens crack front

The two extreme configurations are shown on figure 7. The crack front is either parallel to the flaw pattern (Fig. 7a), or either perpendicular (Fig. 7b). A simple electrical analogy can be made considering FIA as a stacking of two types of band of matter: one with poor FCG resistance, the other with high FCG resistance, whatever the reason of the differences. Schematic case (a) can be compared to a series connecting and case (b) to a parallel connecting. Hence, for a same volume fraction of "good" and "bad" material, FCGR is higher for case (a) than for case (b), the crack steadily interacting with the material microstructure in the latter case.

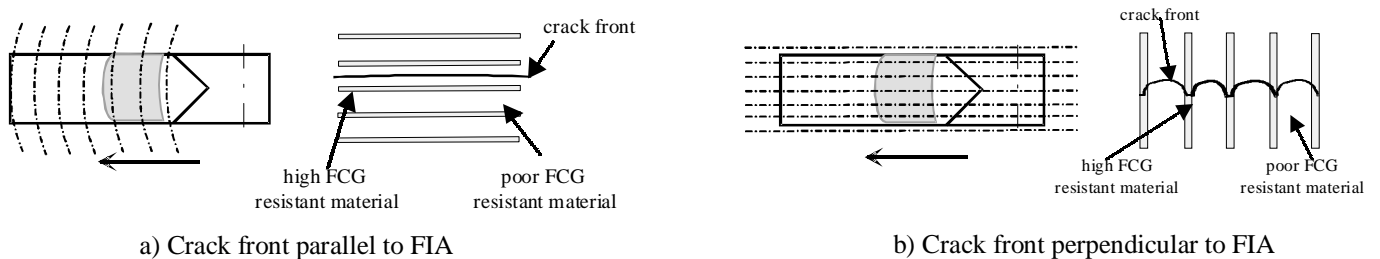


FIG. 7 : CRACK FRONT POSITION VERSUS PATTERN FLOW FOR CT SPECIMEN

Position A specimens reported in figure 5 correspond to diagram 7a and produce higher growth rates than position B specimens, which correspond to diagram 7b. Therefore, a simple conclusion can be drawn : For 2D cracks, FCGR are the higher when the crack front is parallel to flaw pattern than when perpendicular to it. For this case, transgranular fracture seems to be favoured by propagating across the δ discs sheets.

4.2 3D KB specimens crack fronts

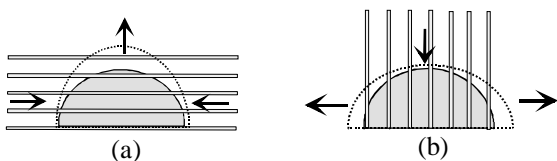


FIG 8 : SCHEMATIC ORIENTATIONS OF CRACK FRONT VERSUS FIA, LEADING TO ARRANGEMENT OF CRACK ASPECT RATIO.

Considering radial and axial oriented specimens, the analysis is more complicated for a semi-elliptical crack crossing the FIA, as shown in figure 8. On diagram 8a, at the depth of the crack, the crack front is parallel to the δ discs sheets, which should lead to intergranular fracture and high rates. However, near specimen surface, crack front is perpendicular to FIA, which is expected to produce low rates and mixed mode fracture. Diagram 8b shows the opposite configuration. Hence the global growth rate of the crack appears to be difficult to predict.

Figure 8 can also explain the observed differences in crack front aspect ratio α . For semi-elliptical cracks, several parameters can influence aspect ratio α . Considering isotropic crack growth material, with no crack closure effect, uniform loading along the crack front ($\Delta K=cte$ wherever) should theoretically lead to $\alpha=a/c<1$. Taking into account crack closure effects this ratio is close to 1 (see e.g. [7]), slightly decreasing as a/t increases. Environment and fracture modes play a major role as well. When time dependent fracture mode is operating, tunnelling effect can be observed which produces higher growth in the depth of the specimen than on the surface. This has clearly been observed recently on longer cracks in 718 alloy at 600°C [8] : under air conditions, crack profiles adopt a tunnelled shape to reach $\alpha>1$ and fracture mode is intergranular. Under high vacuum, crack profile tends to 0.8, the fracture being fully transgranular. This behaviour can be supposed to enhance modification of aspect ratio caused by crack orientation. At the crack depth of case 8a, rapid intergranular fracture occurs which should causes tunnelling effect whereas on

surface slow rates are expected. Indeed, for radial KB specimen exhibiting high global rates and this orientation, α has been shown to be superior to 1.3. The opposite situation of diagram 8b is confirmed by the observation of axial KB crack front, which produced global lower rates and aspect lower ratio $\alpha < 1$.

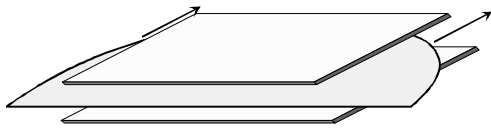


FIG 9 : CRACK GROWTH BETWEEN SHEETS OF δ PEBBLES.

The last possible configuration is when crack front is growing between the sheets, as shown on figure 9. Since δ precipitates for a large fraction at grain boundaries, crack is then expected to be fully intergranular with high rates. This configuration corresponds to tangential KB specimens. Figure 6 confirms that FCGR is the higher with this orientation while aspect ratio α is measured close to 1.2. In this case, the crack does not cross FIA sheets, so that

crack tunnelling effect is only due to classical environmental effects. α values are here comparable to those measured at 600°C [8].

Concerning fracture mode, figure 10 confirms intergranular cracking and the major role of δ phase on "guiding" the crack growth. Indeed, broken grain boundaries are covered of cellular δ .

Hence δ phase orientation and distribution seems to be the most important factor of FIA to consider when dealing with crack growth rates and crack path.

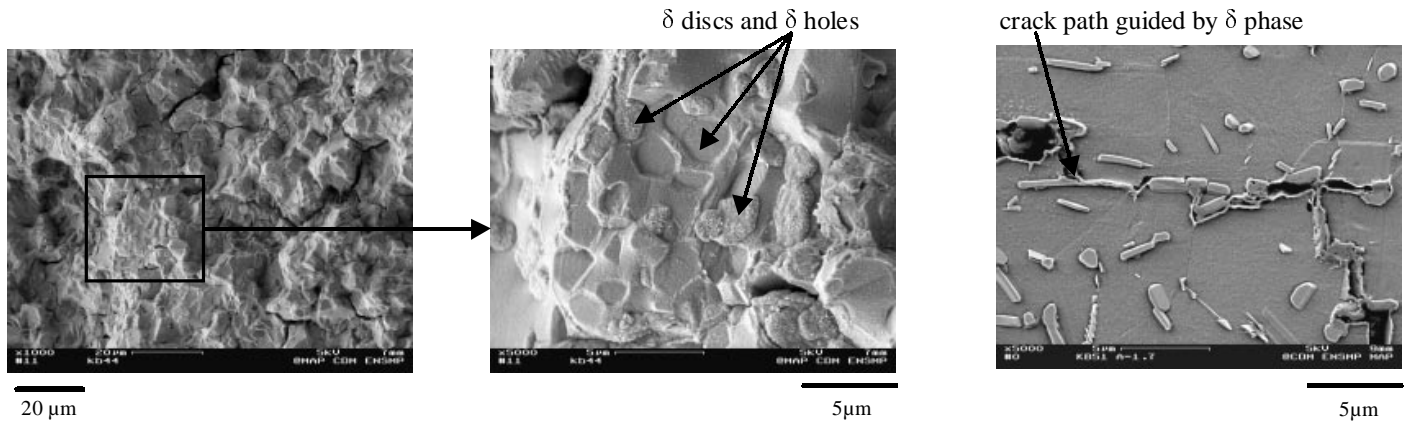


FIG 10 : CRACK GROWTH BETWEEN FIA SHEETS : FULLY INTERGRANULAR FRACTURE, CRACK PATH GIVEN BY δ ARRANGEMENT.

4.3 Usefulness of δ phase in the alloy

Considering the results of the present study, the question of the usefulness of δ phase in alloy 718 regarding FCGR in creep fatigue conditions is still open. Answer seemed to be given by a study on two Direct Aged In 718 discs [9]. In this study, the comparison was made between 2 discs differing only by δ phase proportions. It was shown that the disc with the larger proportion of δ phase has better resistance to creep initiation and creep-fatigue crack growth. Globular δ distribution at grain boundaries seems to have a retardation effect on FCGR and to postpone intergranular crack propagation. That study concluded on the usefulness on δ if the proportion of this phase is well controlled.

The present study brings further explanations on this point. δ phase plays a complex role on FCG resistance of industrial parts. This paper shows that huge effects on FCGR are induced by the orientation of crack front according to δ arrangement. When the crack front is perpendicular to δ alignments, δ presence is useful leading a change of fracture mode. When the crack grows between δ alignments, intergranular fracture is enhanced and FCGR are dramatically high. Hence, δ appears to be particularly useful only if its arrangement in the component may allow crack retardation in its critical zones. These observations are not contradictory to those on DA718 discs because in this case, the crack seems to cross δ alignments.

5 CONCLUSIONS

Four main observations and conclusions can be drawn from this study :

- Forming conditions and involved pattern flaw may have drastic effects on the fatigue resistance of components tested under high temperature creep-fatigue cycles.
- When a crack propagates between δ phase alignments, high rates associated with intergranular fracture mode are enhanced. When a crack has to cross FIA perpendicularly, retardation effects can be observed and mixed mode fracture involving partially transgranular fracture can occur.
- If the arrangement of δ phase is well controlled by forming operations, the presence of this phase in critical zones of a component could improve its FCG resistance.
- This study underlines the importance of performing tests on real industrial parts.

ACKNOWLEDGEMENTS

Authors would like to acknowledge SNECMA for its industrial support and collaboration for this study.

REFERENCES

1. Ghonem H., Nicholas T. and Pineau A. (1993), *Fatigue Fract. Engng. Mater. Struct.* **16**, N° 5, p 565 and **16**, N° 6, p 577.
2. Pineau A. (1997), In : *Engineering Against Fatigue (Ed. J.H Beynon, M.W. Brown, R.A. Smith T.C. Lindley & B. Tomkins)*. Chap 60, p 557.
3. Floreen S. and Kane R. H. (1980), *Fatigue. Engng Mat. Struct.* **2**, .p 401.
4. Khobaid M., Ashbaugh N. E., Hartman G. A., Weerasooria T., Maxwell D. C. and Goodman R. C. (1988), *AFWAL-TR-88-4062* Wright-Patterson AFB, OH, May.
5. Pédrón J. P. and Pineau A. (1982), *Mat. Sci Engng.* **56**, p 143.
6. Newman J.C. Jr and Raju I.S. (1981), *Engng. Fract. Mec.* **15**, N°1-2, p185
7. Jolles M. and Tortoriello V. (1983), *In Fracture Mechanics: Fourteenth Symposium-Volume I: Theory and Analysis, ASTM STP 791 (Eds J.C. Lewis and G. Sines)* p I-297
8. Bache M.R., Evans W.J and Hardy M.C. (1999), *Int. J. Fatigue* **21** p S69
9. Shuqi L., Jingyun Z., Jinyan Y., Qun D., Jinhui D., Xishan X., Bing L., Zhichao X., Zhen C., Zhaoqian S. and Cizheng J., (1994), *Superalloys 718, 625, 706 and Various Derivatives (Ed, E.A. Loria)*. The Mineral, Metal & Materials Society, p 545.